

**BULK LIFETIME ENHANCEMENT BY FIRING STEPS
IN BACK CONTACTED MULTICRYSTALLINE SILICON SOLAR CELLS**

Rafel Ferré¹, Nils-Peter Harder^{1,2}, Wolfgang Mühleisen¹, Sandra Herlufsen¹, Christian Ulzhöfer¹, Martin C. Schubert⁴, Robert Wade⁵, Verena Merten⁵, and Rolf Brendel^{1,3}.

¹Institute for Solar Energy Research Hamelin (ISFH), Am Ohrberg 1, 31860 Emmerthal, Germany.
Tel +49(0)5151 999 413, e-mail: ferre@isfh.de

²Institut für Materialien und Bauelemente der Elektronik, Leibniz University of Hanover, Schneiderberg 32, D-30167 Hannover, Germany

³Institute of Solid-State Physics, Leibniz University of Hannover, Appelstrasse 2, D-30167 Hannover, Germany

⁴Fraunhofer Institute of Solar Energy Systems, Heidenhofstrasse 2, 9110 Freiburg, Germany

⁵Q-Cells SE, Sonnenallee 17-21, 06766 Bitterfeld-Wolfen (OT Thalheim), Germany

ABSTRACT: We study bulk lifetime enhancement of *p*-type multicrystalline silicon (mc-Si) wafers for back contacted solar cells, in particular Emitter-Wrap-Through (EWT). We perform 55 Ω/sq phosphorus diffusion to getter metallic impurities and firing of silicon nitride (SiN) to induce hydrogen passivation. We analyse the bulk passivation in four scenarios that can occur simultaneously in the wafer: (a) firing of gettered areas with emitter (b) firing of gettered areas after removing the emitter, (c) firing of not gettered (not diffuse(d) areas and (d) firing with single side side emitter diffusion. Scenario (a) enhances strongly the lifetime of the wafer bulk, whilst (b) and (d) reduce it slightly. Scenario (c) produces strong degradation of the bulk lifetime.

1 INTRODUCTION

A critical parameter in the production of high-efficiency back-contacted multicrystalline silicon solar cells is the enhancement of the bulk minority carrier lifetime. This ensures a sufficiently high diffusion length of the minority carriers in order to reach the rear contacted emitter. Emitter diffusion followed by Plasma Enhanced Chemical Vapour Deposited (PECVD) silicon nitride (SiN) coating and short firing at high temperatures provide gettering of metallic impurities and hydrogen bulk passivation, respectively. Additionally, the fired SiN layers have to ensure surface passivation, unless they are removed to deposit afterwards a new layer.

with the rear-side metalized emitter. This partially compensates the impact of a short diffusion length of the bulk.

Depending on the design of the cell, three scenarios may occur in the wafer: (a) firing of gettered areas with *n*⁺-emitter, (b) firing of gettered areas after removing the emitter, and (c) firing of not gettered (not diffused) areas.

Figure 1 shows two different sequences for the manufacture of an EWT solar cell. In sequence A, the entire surface of the wafer is diffused (and therefore gettered) and afterwards partially removed to define the *p*-type finger at the rear side. Then, a silicon nitride passivation layer is coated by PECVD and fired. During the firing scenarios (a) and (b) occur. On the other hand, in possibility B, an etching barrier is coated before the diffusion, thus defining a priori the *p*-type finger. Once the etching barrier is removed, the silicon nitride is deposited and fired. Therefore, in this case the scenarios (a) and (c) are present. Note that in process B the situation is different to the scenario (d), in which the emitter is only diffused on one side of the wafer.

In this work, we demonstrate that the scenarios (a), (b), (c), and (d) as well as the emitter coverage fraction affect strongly the bulk lifetime and therefore the final solar cell efficiency.

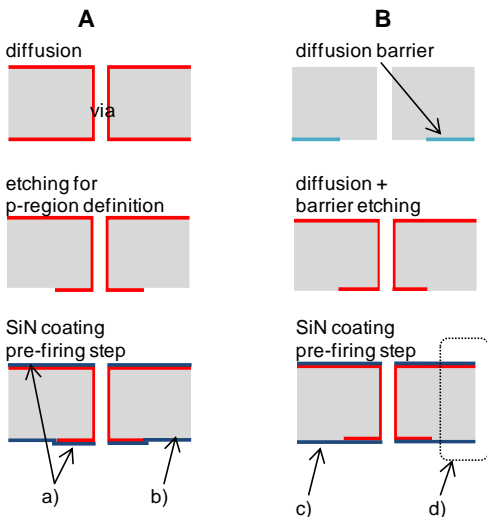


Figure 1: Two process sequences for an EWT solar cell before firing for hydrogen passivation of the bulk. Although A and B result in the same cell structure, the differences in the processing lead to different scenarios.

A particular concept of back contacted cells, the Emitter-Wrap-Through (EWT) cell, is conceived to collect the carriers produced near the front side through phosphorus-doped vias, connecting the front side emitter

2 EXPERIMENTAL DETAILS

Neighbouring *p*-type mc-Si wafers with resistivities between 1 to 2 Ω cm are saw damage etched and RCA cleaned. We perform different variations in our experiment in order to explore the scenarios (a), (b), (c), and (d) separately. For scenario (a) we perform a POCL₃ phosphorus diffusion with an emitter sheet resistance of 55 Ω/sq followed by a 30 h internal gettering at 500 °C [1]. Then we deposit 100 nm of hydrogenated PECVD-SiN layers with refractive index *n* = 2.05 at a 632 nm wavelength. For scenario (b) an emitter etching step is added after the internal gettering. For scenario (c) the wafers are fired without diffusion and internal gettering. With respect to the final structure, scenario (d) is the same as (a), however, in the fabrication process of (d) a diffusion barrier (SiN *n* = 1.9, 100 nm) prevents the

diffusion on one side of the wafer and subsequently this diffusion barrier is removed.

In order to analyze the impact of the emitter coverage fraction on the lifetime we prepare wafers with selective diffusion barriers of different widths on both sides of the wafers. The structuring of the barrier is performed by ablating the silicon nitride locally by a picoseconds laser and a damage etching step.

We perform the firing steps in a conveyor furnace, determining the temperature profile as a function of the time with a K-type thermocouple attached on a silicon wafer. The firing takes a total time of around 90 s with a pre-plateau of 500°C for 20 s and a peak temperature of 700 °C for approximately 2 s.

Finally, we etch off the first 5 μm from both sides of all wafers with CP4 acidic etch, RCA clean, and re-passivate with a high-quality silicon nitride coating with a refractive index of 2.4 at 632 nm. Afterwards, lifetime measurements using Infra Red Steady State Photo Conductance (IRSS-PC) [2] and Photoluminescence (PL) [3] measurements follow.

3 FIRING UNDER DIFFERENT SCENARIOS

Figure 2 shows the injection-dependent effective lifetime measured by IRSS-PC on the etched and re-passivated wafers. Before thermal treatment the wafers show already high electronic quality with lifetimes around 200 μs . The emitter diffusion enhances the lifetime up to 300 μs . A subsequent silicon nitride coating followed by firing, i.e. scenario (a), produces a strong benefit with lifetime values up to 500 μs . However, if the emitter is totally removed [scenario (b)] a firing step is not recommended, as the bulk lifetime degrades at injection densities below 10^{15} cm^{-3} . Firing the wafer without any previous diffusion [scenario (c)] produces a strong degradation of the wafer quality over the entire injection range and, hence, should be avoided at all.

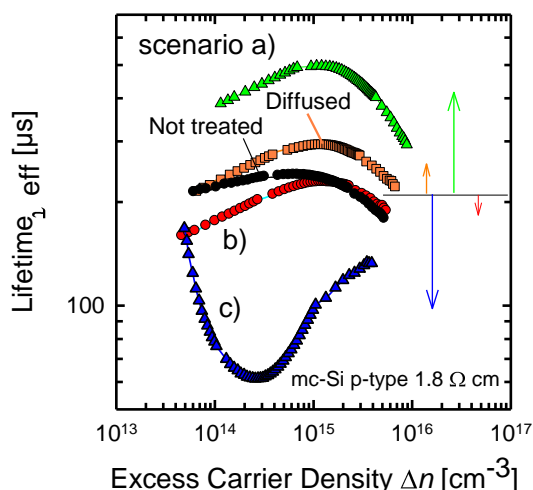


Figure 2: Effect on the bulk lifetime after firing mc-Si wafers under scenarios (a) with n^+ -emitter, (b) after etching the n^+ -emitter, and (c) without n^+ -emitter diffusion.

The effect of single-side vs. two- sides emitter diffusion, i.e. corresponding to scenario (d), is shown in Fig. 3. Already before firing, wafers with both sides

diffused emitter show higher bulk lifetimes, probably attributed to a better gettering effect. After firing the differences are much more pronounced, leading to degradation in the case of single-side emitters and an improvement for the wafers diffused on both sides. Additionally, we observe that statistically there is a higher scattering in the measurements for single-side emitters (not shown in the graph).

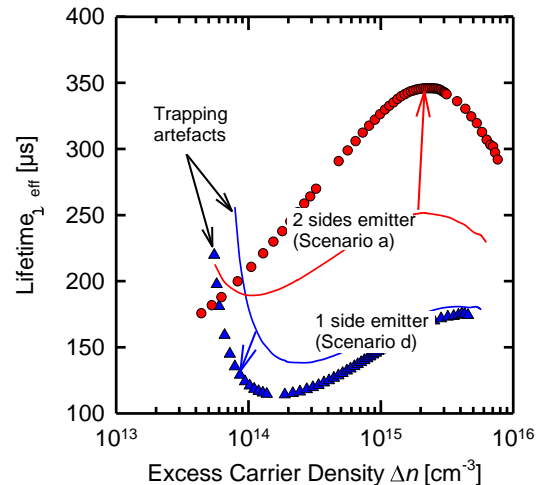


Figure 3: Bulk lifetime of wafers with 1-side and 2-side n^+ -emitter diffusion before firing (solid lines) and after firing (symbols) and the impact of trapping effects.

The physical mechanism responsible for the different final bulk lifetimes after firing is, to our best knowledge, unknown. A possible explanation could be the technological details of processing. During firing the silicon nitride and the emitter may act as barrier against external contamination, namely metallic impurities coming from the belt furnace walls. The phosphorus diffused emitter is an excellent gettering region, either due to a much higher solubility of the metallic impurities in this region than in the wafer bulk, or to the production of large amounts of self-interstitials in silicon acting apparently as gettering sites [4]. In any case, for scenario (a) the bulk is covered by a thick gettering barrier which is subsequently removed. We shall adopt here the view that this gettering layer serves as a protection against external contamination; however we do also acknowledge the possibility that processes within the wafer lead to different results upon firing with an d without a gettering layer at the surface. We therefore envisage the bulk as being not affected by external contamination in scenario (a), but receiving beneficial hydrogen defect passivation. In scenario (b) the extra gettering barrier is not present anymore, but a certain amount of metal impurities were gettered previously in the etched-off n^+ -emitter. Once this emitter is removed, impurities are not available to be re-injected in the bulk during the firing. This would explain the relatively small lifetime reduction observed in Figure 2 without suffering from strong degradation like in scenario (c). In that case the wafer receives an extra amount of metallic impurities during the firing (or, in the alternative view: the wafer suffers from renewed release of metal atoms from precipitates during firing without simultaneously gettering by an emitter). This causes additional recombination centres and degrades the carrier lifetime in the bulk significantly. Finally, scenario (d),

corresponding to the single-sided emitter case, can be re-interpreted as a mixture of (a) having a gettering barrier, and (b) having no gettering barrier but thermal treatment (i.e. gettering) applied.

In the IRSS-PC measurements we observe the presence of artefacts at low injection range coming from non-recombination trapping centres in the bulk [5] or Depletion Region Modulation (DRM) due to the band bending at the surface caused by the SiN passivation [6]. In addition, the position of these artefacts in the Δn axis is not constant, but depends on the lifetime level. Actually, for curves with lifetimes above 300 μs these artefacts are not observed, probably because they are at Δn values lower than those offered by the measurements.

According to the trapping model of Hornbeck and Haynes [7,8] and the description of MacDonald and Cuevas [9], the position of the artefact depends only on the trap density. Correspondingly, the position of the artefact in the DRM effect is independent of any other parameter not linked to the surface. Since all wafers are equally passivated we attribute the different positions of the observed “tails” of increased apparent lifetime to different trapping concentrations. Consequently, the density of these two types of centres might be correlated and both of them can be passivated by hydrogen. Another possibility was suggested recently by Harder et al. [10, 11], who used the Shockley-Read-Hall (SRH) recombination statistics [12,13] for describing trapping artefacts. Such model has been successfully used by MacIntosh et al. [14] for describing the temperature dependence of trapping effects. In this approach it is acknowledged that trap states are likely to also exhibit non-zero (yet very small) carrier capture cross sections for majorities; and thus these traps will also give rise to SRH recombination. This provides a natural way to link trapping artefacts with low recombination lifetime, which are often found to correlate such as in our samples here.

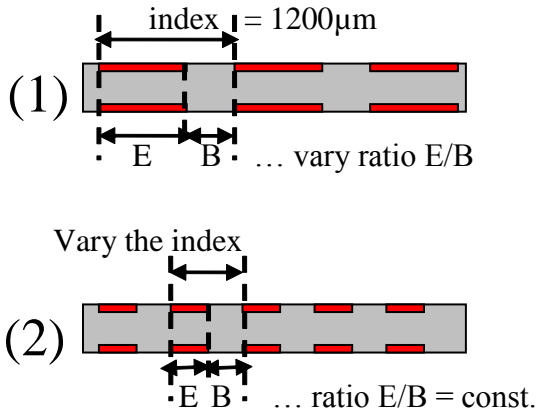


Figure 4: Sample structures with varying emitter structures: (1) keeps the index constant and varies the emitter coverage fraction, and (2) keeps the emitter coverage fraction constant (50%) and varies the index.

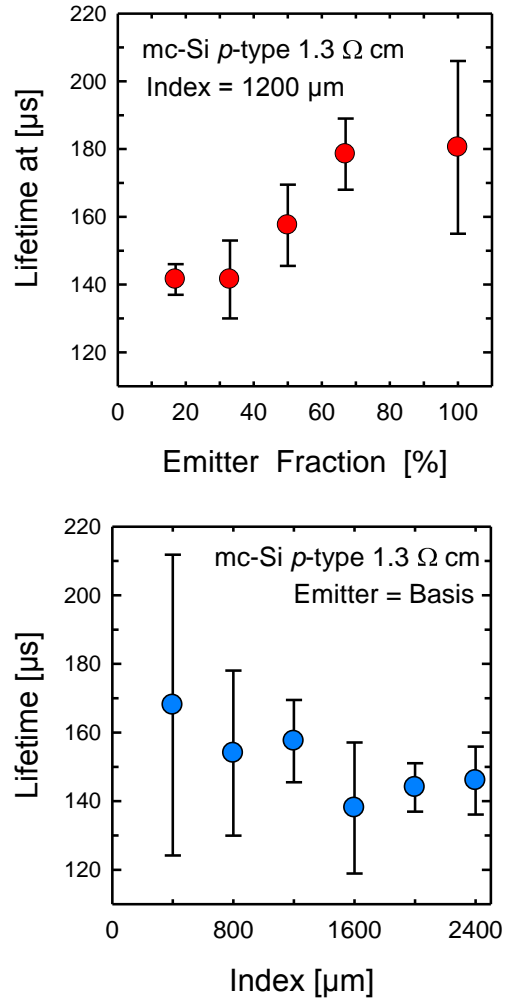


Figure 5: Influence of the emitter coverage fraction during the firing on the final bulk lifetime (measured at $\Delta n = 5 \times 10^{14} \text{ cm}^{-3}$). Top: fixed index varying the emitter fraction. Bottom: variation of the index with the same emitter-to-base coverage.

4 INFLUENCE OF EMITTER COVERAGE

Typically, back contacted solar cells have an index (distance between two fingers of the same type) between 800 to 1500 μm . The fraction of the emitter area may vary according to the design used. To clarify the influence of the emitter coverage on the final bulk lifetime after firing, we apply selective diffusions on both sides of the wafer and prepare samples with emitter geometry variations as shown in Figure 4. The samples were further processed as our previous lifetime samples: SiN-coating after emitter preparation, Firing, etching of the SiN, etching of the emitter, and re-passivation of the surfaces with a passivating SiN with refractive index $n=2.4$. Figure 5 shows the results of the corresponding lifetime measurements. For a constant index of 1200 μm , the bulk lifetime increases monotonically with the emitter coverage fraction, as depicted in Fig. 5 (top), up to a certain saturation at around 60 to 70%. For a constant emitter-to-base area ratio (Fig. 5, bottom) we observe a slight decrease of the passivation for increasing values of the index. This effect is plausibly explained by the reduced likelihood of impurities to reach the gettering

sites in case of small emitter coverage fractions on the one hand. On the other hand, in case of a large index, the distances in between the emitter regions may be too wide to benefit from the neighbouring emitter regions. However, it may be difficult to explain these findings exclusively in terms of path lengths for impurities towards the nearest emitter regions, otherwise our previously investigated samples with a single-sided emitter would have been able to yield very good lifetimes: In the single-sided emitter sample each position in the wafer is only less than 200 μm away from the emitter, yet does not yield the same relatively high lifetimes as the 50% emitter coverage fraction for small index. This consideration strengthens the hypothesis that the emitter layer serves also as a “barrier” against external contaminants during the firing process.

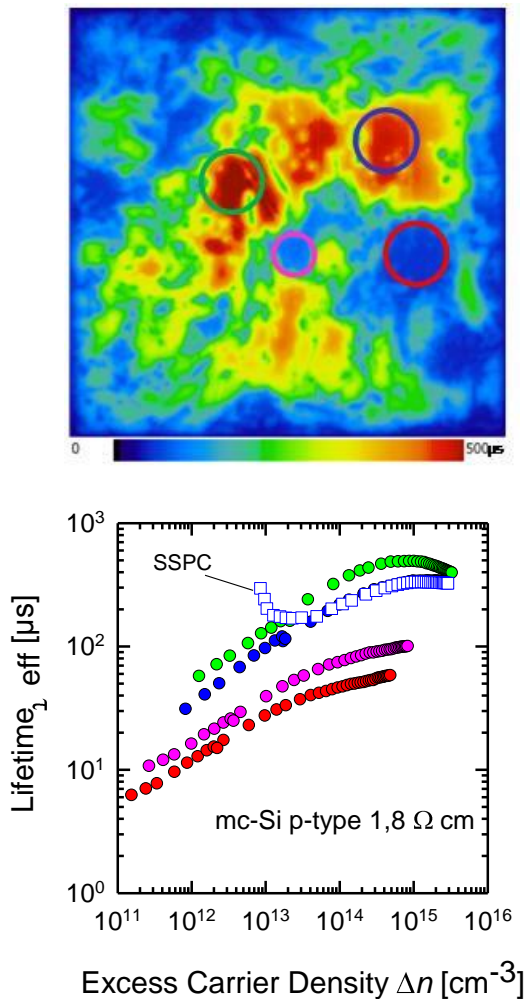


Figure 6: Top: Photoluminescence lifetime image at 0.8 suns in a gettered and fired wafer, corresponding to scenario (a). Bottom: Lifetime injection dependence for 4 different regions marked in the mapping. Open circles are SSPC measurements for lifetime calibration of the PL measurements.

5 V_{oc} LIMITS IN EWT CELLS

In order to determine the real lifetime at low injection density we perform photoluminescence measurements. Fig. 6 shows the spatially resolved PL of a wafer processed according to scenario (a) at a fixed

illumination intensity of 0.8 suns, together with the lifetime injection dependence for selected areas. Although some regions show very high lifetime values (up to 500 μs) at around $\Delta n \approx 10^{15}$ cm^{-3} there are two issues to take into account. First, the injection dependence is very strong. Second, some regions show poor lifetimes even after the best treatment. The values to take into account for an operating solar cell are those corresponding to the maximum power point, i.e. $\Delta n \approx 10^{12} - 10^{13}$ cm^{-3} . In our measurement the corresponding lifetime values lay between 10 and 100 μs .

We finally estimate the limits of the open-circuit voltage V_{oc} and efficiency of hypothetical (EWT) solar cell made of our lifetime samples. For this purpose we use the spatially resolved lifetime dependence as measured by photoluminescence and displayed in Fig 6. To this end we consider single (separate) diodes for regions with equal lifetime that are conceived to be interconnected in the complete hypothetical solar cell. For each of these constant-lifetime regions we derive the implicit voltage as a function of excess carrier density and use the lifetime data and thickness of the sample to calculate corresponding bulk recombination rates. Those values can be used to determine bulk I-V characteristics. We furthermore associate with the various surface regions depicted in Figure 1 recombination currents that are characterized by saturation current densities J_0 . In this way we calculate the local recombination current densities (given for example in A cm^{-2}) for the passivated front side emitter and the via, as well as for the base, base contacts and metallized emitter fingers. Then, we scale the corresponding contributions with an area factor and determine the recombination current densities *per cell unit area* (i.e. $\text{A cm}^2/\text{cell}$). The parameters used in our simulations are summarized in Table 1. Once we have determined in this way the dark I-V curve for one diode, we assume all diodes working in parallel and sum all the contributions with the relative frequency of the various material qualities. For this purpose we estimate the area fractions of a selected set of representative lifetime regions from the PL image in Figure 6. Finally, we calculate the light I-V curve by assuming a short-circuit current of the complete hypothetical solar cell: $J_{sc} = 38$ mA/cm^2 . For the Efficiency calculation we assume an additional external resistance of 0.8 Ωcm^2 .

Figure 7 plots calculated open-circuit voltage limits as a function of the area fraction between two different regions, one with a high-quality material (160 μs at $\Delta n = 10^{13}$ cm^{-3}) and another one with poor quality material (30 μs at $\Delta n = 10^{13}$ cm^{-3}), each with the corresponding injection dependence as depicted in Figure 6.

In the same manner than the V_{oc} plot of Figure 7, Figure 8 plots the efficiency of the hypothetical solar cell as a function of the area fraction between two different regions, one with a high-quality material (160 μs at $\Delta n = 10^{13}$ cm^{-3}) and another one with poor quality material (30 μs at $\Delta n = 10^{13}$ cm^{-3}), again each with the corresponding injection dependence as depicted in Figure 6.

We estimate the V_{oc} limit for the wafer measured in Figure 6, assuming to have four different regions as indicated in Table 1. For this particular wafer we calculate an open circuit voltage of as 638 mV, indicating the possibility of performing high-efficiency EWT solar cells using mc-Si wafers.

Table 1. Top: Parameters for calculation of V_{oc} limits in a EWT cell as a function of bad to good area ratio. Bottom: calculation for a wafer assuming four regions (Figure 6) with

$J_{0,EWT-via}$	33 fA cm ⁻² /Cell
$J_{0,E,front}$	200 fA cm ⁻² /Cell
$J_{0,E,back}$	300 fA cm ⁻² /Cell
$J_{0,Basis}$	125 fA cm ⁻² /Cell
J_{sc}	38 mA cm ⁻²
W	160 μm
N_A	8x10 ¹⁵ cm ⁻³
Bad lifetime	160 μs ($\Delta n = 10^{13}$ cm ⁻³)
Good lifetime	30 μs ($\Delta n = 10^{13}$ cm ⁻³)
Wafer (% are(a))	τ at $\Delta n = 10^{13}$ cm⁻³
Region 1 (10%)	160 μs
Region 2 (25%)	30 μs
Region 3 (20%)	100 μs
Region 4 (45%)	40 μs
V_{oc} limit	638 mV

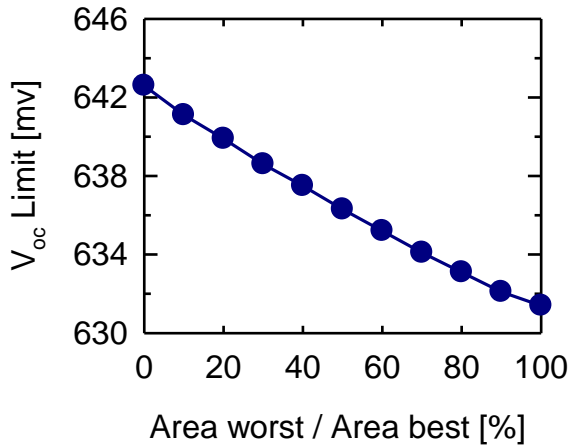


Figure 7: Open-circuit voltage limits for the hypothetical solar cell made from our lifetime sample in Figure 6. The x -axis varies the relative contribution (area coverage) of the best and the worst lifetime region. The V_{OC} values are calculated under the assumption of surface-related saturation current contributions as given in Table I and under further assumption of a $J_{SC} = 38\text{mA}/\text{cm}^2$.

6 CONCLUSIONS

We showed that different preparations of the emitter diffusion for back-contacted mc-Si solar cells influence strongly the hydrogen passivation of the bulk by means of firing. Firing in the presence of a diffused n^+ -emitter on both sides of the wafer substantially enhances the bulk lifetime, whereas firing once the emitter is etched off reduces it slightly. On the other hand, firing without any previous diffusion deteriorates strongly the bulk lifetime. In addition, the bulk lifetime after firing increases monotonically with the emitter coverage fraction.

Spatially resolved photoluminescence was used to determine the lifetime distribution and calculate a limit of the open-circuit voltage for a particular wafer of 638 mV. In the light of these results mc-Si solar cell efficiencies in excess of 18% seems to be viable.

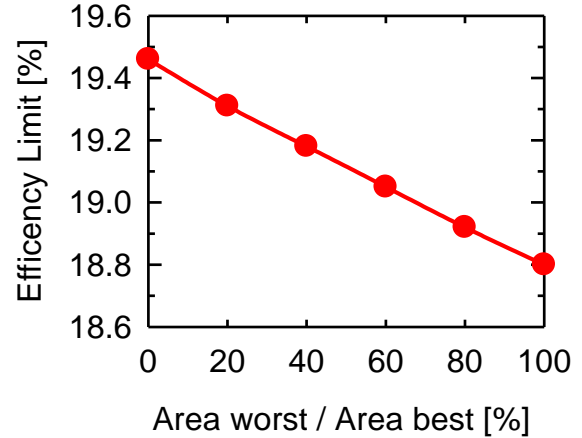


Figure 8: Efficiency estimations for the hypothetical solar cell made from our lifetime sample in Figure 6. The x -axis varies the relative contribution (area coverage) of the best and the worst lifetime region. The V_{OC} values are calculated under the assumption of surface-related saturation current contributions as given in Table I and under further assumption of a $J_{SC} = 38\text{mA}/\text{cm}^2$ and an external series resistance of $0.8 \Omega\text{cm}^2$.

7 ACKNOWLEDGEMENTS

This work was funded by the German State of Lower Saxony and the German Federal Ministry for the Environment, Nature Conservation, and Nuclear Safety (BMU) under contract no. 0329988C (ALBA II).

REFERENCES

- [1] R. Krain et al, Appl. Phys. Lett. **93**, 152108 (2008)
- [2] R. A. Sinton and A. Cuevas, Appl. Phys. Lett. **69**, 2510 (1996)
- [3] S. Herlufsen, J. Schmidt, D. Hinken, K. Bothe, and R. Brendel, Phys. Stat. Solidi (RRL) **2**, 245 (2008)
- [4] W. Schroter and R. Kuhnappel, Appl. Phys. Lett. **56**, 2207 (1990).
- [5] D. Macdonald, PhD Thesis, Australian National University (2001)
- [6] M. Garín, I. Martín, S. Bermejo, and R. Alcubilla, J. Appl. Phys. **101**, 123716 (2007)
- [7] J.A. Hornbeck and J.R. Haynes, Phys. Rev. **97** (1955) p. 311
- [8] J.A. Hornbeck and J.R. Haynes, Phys. Rev. **100** (1955) p. 606
- [9] D. Macdonald and A. Cuevas, Appl. Phys. Lett. **74** (1999) p. 1710
- [10] N. P. Harder, R. Gogolin, R. Brendel, Appl. Phys. Lett (submitted)
- [11] R. Gogolin, N.-P. Harder, and R. Brendel, 35th IEEE-PVSC 2010 (Hawaii).
- [12] W. Shockley, W.T. Read, Phys. Rev. **87** (1952) p. 835.
- [13] R. N. Hall, Phys. Rev. **87** (1952) p. 387.
- [14] Keith R. McIntosh, Bijaya B. Paudyal, and Daniel H. Macdonald, J Appl Phys **104**, 084503 (2008)